

Discrete Approaches to Cohesive-Crack Modeling through the Finite Element Method

Túlio N. Bittencourt

*Laboratório de Mecânica Computacional
Laboratório de Estruturas e Materiais Estruturais
Escola Politécnica da Universidade de São Paulo*

Abstract

In this work the application of the fictitious cohesive crack model for two-dimensional problems is explored in the context of the finite element method. Initially, a brief literature overview of the cohesive crack problem is presented. Different strategies to solve the fictitious crack problem in 2D are reviewed and introduced. First, the influence method proposed by Hillerborg *et al.* [Hillerborg 1976 and Petersson 1981] is treated. Then the use of interface elements and the finite element method is considered. A defined crack path approach is detailed. As shown later, the fracture zone propagation is closely associated with the interface constitutive model. Then a new, integrated, arbitrary, cohesive crack propagation strategy is presented. This strategy is based on: interactive, effective total crack (true crack plus fracture process zone) length control, a criterion for propagation based on fictitious crack tip parameters (opening profile, tip stress, or tip singularity), a local principal-stress-based criterion for direction of propagation, a dynamic relaxation solver for determining propagation length, and automatic remeshing to accommodate arbitrary growth. In this new strategy, the user controls the simulation by indicating a total crack growth increment in the predicted direction. The analysis proceeds to determine a load factor associated with this increment. Singular elements are not used at the fictitious crack tip. Rather, non-linear analyses may be performed until the stability condition (zero-slope of the crack opening profile, tip stress equal to tensile strength, or near cancellation of singularity) at the tip is reached. Finally, some examples are presented to illustrate and discuss the accuracy and versatility of the different strategies. The new strategy is shown to be stable via a set of example problems which include Mode I with and without snap-back instability, and curvilinear propagation.

1. Overview

Three different known toughening mechanisms are present during crack propagation in ceramic materials [Shah 1989]: (a) surface energy dissipation, (b) micro cracking, and (c) energy dissipation in the wake of the crack path, such as aggregate interlock and bridging. There is compelling evidence that the most important toughening mechanism in non-transforming ceramics at ambient temperature is energy dissipation in the crack wake [Swanson 1987, Vekinis 1990, Rödel 1990, Llorca 1991, Mai 1991]. In this case, a cohesive crack model (CCM) is usually employed to take into account the softening strain localization phenomenon associated with this dissipation mechanism.

A model, proposed by Hillerborg *et al.* [Hillerborg 1976, Petersson 1981] considers the energy dissipation in the wake of the crack path, while neglecting the other two toughening mechanisms. CCM is the state-of-the-art tool to analyze the fracture behavior of quasi-brittle materials, including concrete, cement-based composites, rocks, ceramics, and ceramic composites.

The applicability of CCM to general mixed-mode conditions has been the focus of recent attention. Throughout the 1980's, Ingraffea *et al.* [Ingraffea 1984a, Ingraffea 1984b, Hellier 1987, Swanson 1991, Wawrzynek 1987, Ingraffea 1987] have employed a strategy of singularity near-cancellation to handle mixed-mode crack propagation, with optional load or crack length control. Crack stability was controlled by iterating on the load or crack length until residual values of stress intensity factors were obtained at the tip of the fictitious crack. Direction of crack propagation was computed using these same residual values. This criterion sometimes failed to predict accurately the critical load to produce crack extension because the singular elements at the crack tip perturbed the stress field in the cohesive zone. Moreover, use of these elements was inconsistent with the assumption of singularity cancellation inherent in the CCM.

- (a) for a given load factor λ , find the process zone size so that the ultimate tensile strength is achieved at the tip of the process zone; or alternatively,
- (b) for a given process zone size, find the load factor λ that would allow the ultimate tensile strength to be achieved at the tip of the process zone.

The approach (b) is used in this work. Due to the arbitrary nonlinear nature of the softening along $S_{\sigma c}$ (Figure 1), a numerical technique is usually employed to solve the cohesive crack problem. A finite element or a boundary element approach is most frequently used to solve the equations of equilibrium.

3. The Influence Method

The fictitious crack model has to be treated numerically in general. Both the finite element method and the boundary element method can be applied to solve the equilibrium equations. However, due to the nature of the softening model that involves tractions and relative displacements, the boundary element method seems to be a more natural way to approach the problem. Petersson [Petersson 1981], however, used the finite element method to define his procedure called here the influence method. In fact, the influence method is independent of the numerical technique used to solve the equations of equilibrium. Crack displacements are considered through superposition. The contribution of each node along the crack path is taken individually as well as any contribution of the applied loads. The complete crack path is considered initially (Figure 2). This is a strong limitation since the crack trajectory needs to be known *a priori*. General boundary conditions are assumed with proportional loading.

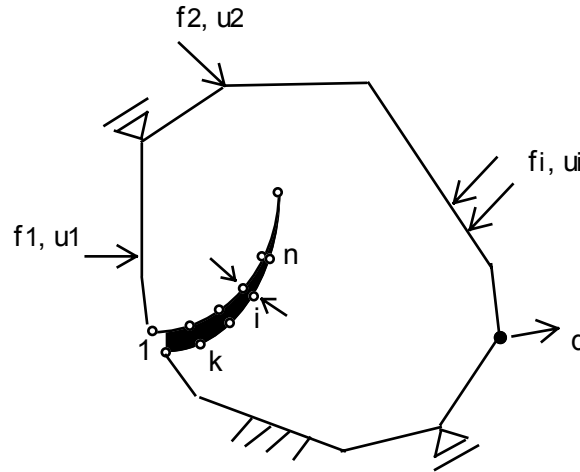


Figure 2 - Discretized cohesive crack problem.

The opening of each node set along the crack is computed for applied opposite tractions or forces (depending on the numerical technique involved) at each node set on the crack path. The opening of each node set for the applied loads is also computed:

$$\mathbf{w} = \mathbf{\Omega} \mathbf{p} + \mathbf{h} F \quad (3)$$

Where $\mathbf{w}(n)$ is the vector of crack openings, $\mathbf{\Omega}(n:n)$ is the influence matrix of crack tractions or forces, $\mathbf{p}(n)$ is the crack traction or force vector associated to the cohesive model, $\mathbf{h}(n)$ is the influence vector of the applied loads, and F is a load factor (scalar). Any response of the body can be obtained by superposition of the influence quantities, for example the displacement d (Figure 2) is obtained as:

$$d = \mathbf{d} \cdot \mathbf{p} + d_F F \quad (4)$$

where \mathbf{d} is the influence vector of the cohesive tractions or forces, and d_F is the displacement due to the applied loads. Proportional loading is controlled by the load factor F .

The advantage of this method is that the equilibrium problem is decoupled from the crack problem. The non-linearity is considered only in the crack problem. By moving the fictitious crack tip along the defined crack path, one can model propagation and compute a load factor associated to each crack configuration. The computation of the load factor must satisfy a stability criterion for the fictitious crack tip.

Suppose that an initial notch is introduced from node 1 to k (Figure 2). In this case, node k defines the true tip of this notch. The fictitious crack tip is then allowed to go from node $k+1$ to node n . Suppose that the fictitious tip is moved to node i while the true tip is still defined by node k . The problem can be solved if the softening model defining the cohesive behavior is known. The goal is to find the load factor F , the traction or force and the opening at each crack node associated to the specified fictitious crack tip position. A boundary element approach will be assumed from this point on. The modifications to consider finite elements are straightforward and the same ideas can be used. Equation (3) can be rearranged when the known crack boundary conditions are introduced:

$$\begin{aligned}
 p_{1\dots k} &= \bar{p}_{1\dots k} \quad \text{and} \quad w_{1\dots k} \text{ is unknown} \\
 p_{k+1\dots i-1} &= g(w_{k+1\dots i-1}) \quad \text{defined by the softening model} \\
 p_i &= f_t \quad \text{and} \quad w_i = 0 \\
 p_{i+1\dots n} &\text{ are unknowns} \quad \text{and} \quad w_{i+1\dots n} = 0
 \end{aligned} \tag{5}$$

where g is a softening function returning traction for a given opening. With the introduction of crack boundary conditions the problem unknowns are reduced to n : the openings of the initial notch ($1\dots k$), the openings of the cohesive zone ($k+1\dots i-1$), the tractions of the elastic zone ($i+1\dots n$), and the load factor F . A nonlinear system equations arises due to nonlinear characteristic of the function g . The solution of such system can be obtained with a Newton-Raphson or a modified Newton-Raphson procedure. The details of that can be found in [Bittencourt 1993]. The traction vector \mathbf{p} , the opening vector \mathbf{w} and the load factor F are then computed for the specified fictitious tip position. An arbitrary response is retrieved by superposition of \mathbf{p} and F . The displacement d , for example, is computed through expression (4). As the fictitious crack tip advances, the specimen responses can be recorded. This is a very useful procedure, but, as said before, it cannot handle arbitrary cohesive crack propagation. The crack path has to be known *a priori*. It should be pointed out that the applied loads may be applied in terms of traction or force as well as displacements.

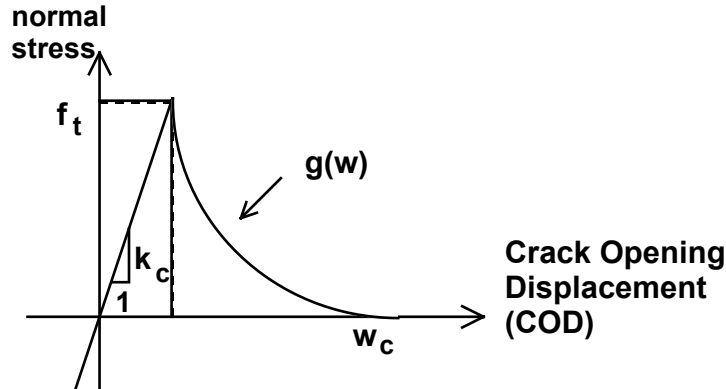


Figure 3 - General softening model of interface elements. The function $g(w)$ is arbitrary.

4. Defined Crack Path Strategy

Another solution of the fictitious crack problem can be obtained through the use of interface elements. The finite element method is considered here. The interface elements [Bittencourt 1993] are associated to a traction-opening model. Thus, if interface elements are placed along the known crack path, a solution can be generated with the Dynamic Relaxation solver. The fracture process zone extension is not controlled by the user in this case. It is closely related to the constitutive model of the interface elements. The position of the fictitious crack tip can be estimated from opening profile. The compressive stiffness (k_c) of the interface model (Figure 3) provides continuity for the constitutive model. This property is crucial for DR. In addition, overlapping of the

crack faces may be prevented by introducing a very large value of k_c . The elastic behavior ahead of the fictitious crack tip can be handled for small values of crack opening.

Preferably, loading is defined through applied displacements because an equilibrium search is performed for each value of the load factor. If applied forces are used, the load capacity of the structure should not be exceeded. If it is, equilibrium may be impossible (Figure 4). In this case the solution is computed under force control and only the increasing force path is computed. Alternatively, a displacement control analysis can be used. For this, it is possible to detect snap-back. Unfortunately, points along the snap-back softening path cannot be obtained. A sudden jump in the force for a small displacement increment indicates the presence of a snap-back condition (Figure 4). The force softening with increasing displacements (Snap-through, Figure 4) is handled appropriately through displacement control.

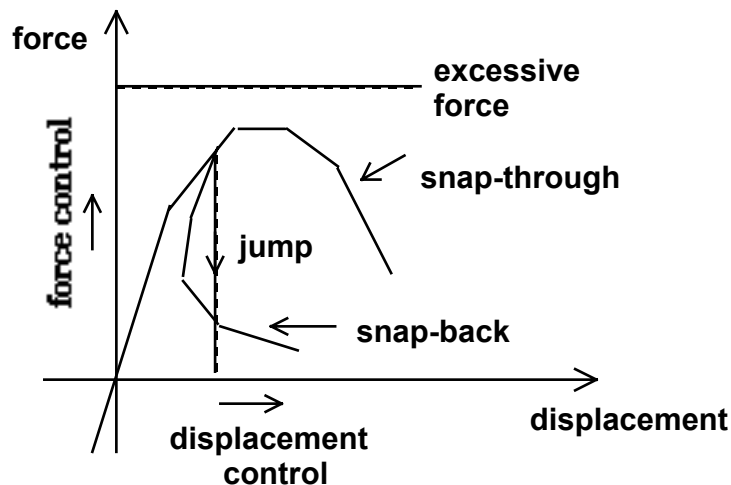


Figure 4 - Possible force-displacement curves.

5. A Strategy for Arbitrary, Cohesive Crack Propagation

In this section an integrated strategy intended to simulate correctly and interactively the evolution of arbitrary, cohesive cracks (ACC) is presented. The term “integrated” emphasizes the first of two innovations described herein: fundamental capabilities for mesh and geometry representation, stress analysis, and non-linear fracture mechanics are combined in a single, engineering workstation-based system. In this context, the use of interactive computer graphics and sophisticated data structures to visualize and control geometry evolution is considered vital. This system is therefore both useful and usable for applied research and solution of practical design and failure analysis problems involving the fracture of concrete.

The second innovation is the introduction of a crack stability criterion based on the fictitious crack-opening displacement (COD) profile. Stability is based on the slope of the crack opening profile at the tip of the fictitious crack. The crack opening gradient must be zero at the tip for a purely cohesive fracture process. This criterion obviates the previous use of singular elements around the tip of the fictitious, cohesive crack. It also provides the most sensitive measure of convergence to simultaneous satisfaction of both global equilibrium and the local traction versus COD constitutive model for cohesive fracture.

The strategy which integrates this new criterion within a friendly and adaptable system is summarized in Figure 5. An important idea is to use self-complete modules for each of the basic elements of the system. The principle of modularity is crucial because it allows one to readily introduce new theoretical, numerical, or constitutive developments. The basic elements of this strategy are described next.

5.1. Fracture Length Control Scheme

It is well known that the load-displacement behavior of cracking ceramic-like structures is size dependent. Strain softening, as well as snap-back instabilities, may occur for the same material depending on structure sizes. Softening can be handled with a displacement control procedure. However, snap-backs are more

difficult to follow. As also recognized by Bocca *et al* [Bocca 1991], snap-back branches can be numerically captured when the loading process is controlled by an increasing function of the fracture process zone (FPZ) length. FPZ length control assures uniqueness of the solution, being a natural and elegant way of handling snap-through and snap-back instabilities. In the present system, the simulation process is controlled through the specification by the user via interactive graphics, of a crack length increment in the predicted direction.

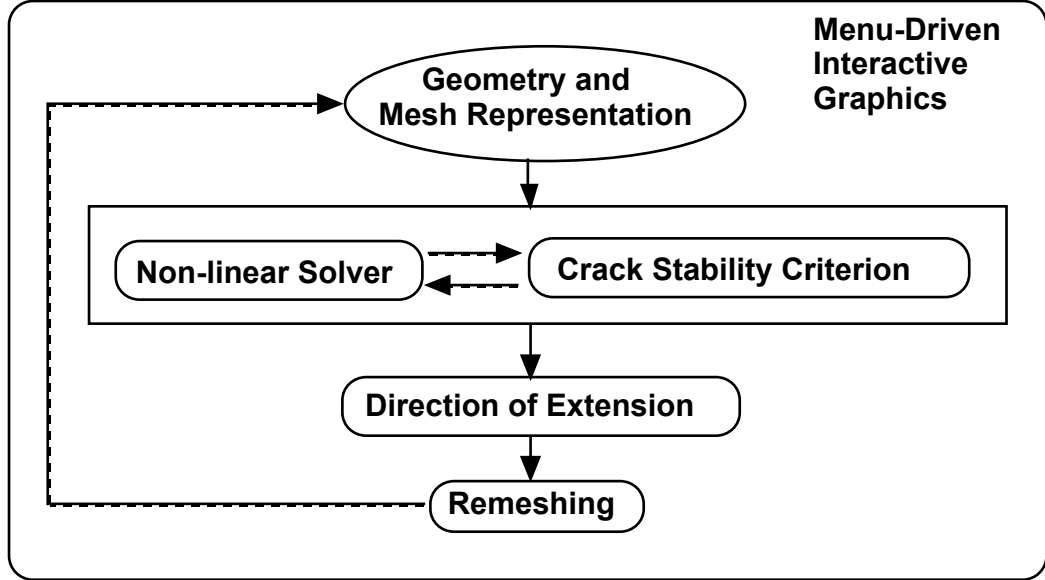


Figure 5 - Integrated strategy for arbitrary, cohesive crack (ACC) propagation modeling.

5.2. Dynamic Relaxation Solver

In the present system, linear elastic quadrilateral and triangular elements are used in conjunction with zero-thickness interface elements in the fictitious crack. The behavior of the interface elements is determined, as previously [Ingraffea 1984a], by non-linear softening constitutive models. Consequently, a non-linear solution technique is required. The dynamic relaxation (DR) technique has been selected for its applicability to potentially highly non-linear problems such as extreme softening and snap-back. A complete description of the solver can be found in [Bittencourt 1993] and reference [Underwood 1983]. DR, although robust, may be slow in some situations, especially when finite elements with large aspect ratios are used. This drawback is reduced here due to the stress-displacement information available from the previous steps of crack propagation. In addition, this explicit solution technique is very attractive for future substantial increases in solution speed via parallel computations.

5.3. Load Factor Computation; Crack Stability Criterion

The objective of this strategy is to determine a loading condition satisfying both global equilibrium and a crack stability criterion for a specified fictitious crack length. Distinct stability criteria that have been used include a tensile strength based criterion [Hillerborg 1976, Petersson 1981], and a fictitious stress singularity cancellation criterion [Ingraffea 1984a, Ingraffea 1984b, Hellier 1987, Swenson 1991].

A criterion based on the fictitious crack tip opening profile is also implemented here. No singular elements are used at the fictitious crack tip. Rather, non-linear analyses are performed until a condition of zero-slope of the COD at the tip is reached. Considering the finite element discretization used here, with linear strain isoparametric elements, the condition of zero-slope can be verified when (Figure 6):

$$\left[\frac{\partial W}{\partial S} \right]_{s=0} = \frac{(4w_B - w_A)}{c} = 0 \quad \text{or} \quad \frac{w_B}{w_A} = \frac{1}{4} \quad (6)$$

where w is the opening of the fictitious crack, and A and B are nodes of the element adjacent to the crack tip. This criterion is implemented in a separate module in the overall simulation system. Although the profile gradient criterion has been applied in the simulations performed herein, the system is not limited to this criterion.

The tensile strength and the singularity cancellation criteria are also available. And more important, others may be introduced readily.

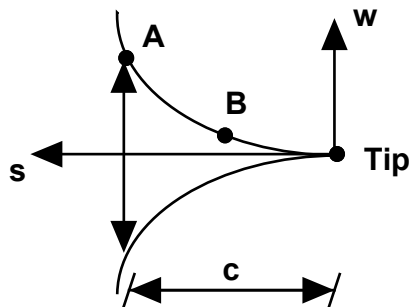


Figure 6 - Zero-Slope Condition of the Opening Profile at the Fictitious Crack Tip.

The next step is to compute the load factor that satisfies the stability criterion for the current fictitious crack length. Monotonic and proportional loading is assumed. Initially, an overestimated value of the load factor is introduced. The dynamic relaxation solver then provides an equilibrated solution for that load factor. The profile gradient at the tip is computed through (6). If the gradient is greater than zero, the load factor is decreased. If the gradient is less than zero, or a closing condition is detected, the load factor is increased. The procedure is repeated until the zero-slope condition is satisfied, within a user specified tolerance.

An important detail of the load factor computation is the initial configuration used in the dynamic relaxation algorithm. The fictitious crack tip is always considered completely open at the beginning of the dynamic relaxation iterations. The cohesive closing forces are introduced within the dynamic iterative process. The last positive gradient configuration is stored and used as the initial configuration for the next candidate load factor. This procedure is necessary to avoid any confusion between admissible configurations in the increasing and decreasing branches of the load-displacement curve, allowing the fracture process zone length control scheme to produce a unique solution.

5.4. Computation of Crack Propagation Direction

When the stability criterion and global equilibrium are satisfied for a given crack or fracture process zone length, the fictitious crack tip is propagated to a new position. The direction of crack extension is defined here by the maximum principal-stress direction due to the remote loading. A numerical search is performed around the fictitious crack tip to determine this direction. The search for maximum circumferential stress is performed along a circle centered at the tip. Here, the search is made along the circle closest to the second layer of Gauss points in the elements surrounding the crack tip. Once the direction is determined, the user graphically indicates the length of the desired increment.

5.5. Automatic Remeshing

Mesh generation can be one of the most time consuming aspects of computational mechanics for moving boundary problems. It is an inevitable step if finite element methods are to be used to model discrete crack propagation. In this case, the mesh must be updated continuously to reflect the changing model geometry. An improved general triangulation meshing algorithm developed by Wawrzynek [Wawrzynek 1991] has been implemented to regenerate automatically the continuum mesh in the present system. A quadtree data structure is used [Samet 1984] together with spatial decomposition and boundary contraction concepts. Simultaneously, additional interface elements are added along the new crack increment. The mesh generation is interactive and requires usually little time to be performed.

6. Example Problems

Two examples are presented to demonstrate the applicability and limitations of the analysis strategies mentioned before. First, a concrete double-edge notched specimen is studied. A single edge notch in bending

(SEN(B)) configuration is considered then. A range of softening responses, including snap-back, is demonstrated for this type of geometry.

6.1. Double-edge-notched Concrete Plate

This example features a double-edge-notched concrete plate specimen (Figure 7) under tension that was tested by Gopalaratnam and Shah [Gopalaratnam 1985]. Although simple, this example displays an illustrative application of the presented distinct numerical strategies to model the cohesive crack problem. Both the defined crack path (DP) and the arbitrary, cohesive crack (ACC) strategies are employed here and the results are compared to the experimental ones. The finite element model takes advantage of the half symmetry of the problem and is depicted in Figure 8.

The nonlinear effects are incorporated into the I6 elements, while a linear elastic behavior is assumed for the Q8 and T6 elements. I6 elements are placed along the line connecting the two notches according to the strategy employed. For DP, interface elements are introduced all along the crack path and the fictitious crack tip is not treated explicitly. In the ACC approach, interface elements are introduced as the fracture process zone evolves. The traction-displacement interface model of the collinear process zone is given by:

$$\sigma = f_t e^{-\nu \cdot \delta} \quad (7)$$

where f_t is the tensile strength of the concrete, ν is a constant that controls the exponential softening, and δ is the COD. Integrating (7) from 0 to ∞ , one can compute the fracture energy:

$$G_F = \frac{f_t}{\nu} \quad (8)$$

By specifying f_t and ν , the fracture energy G_F is defined. G_F for this problem is 0.318 lb/in while the tensile strength (f_t) is assumed to be 525 psi. The elastic modulus equals 4.85e+6 psi and the Poisson's ratio is 0.2.

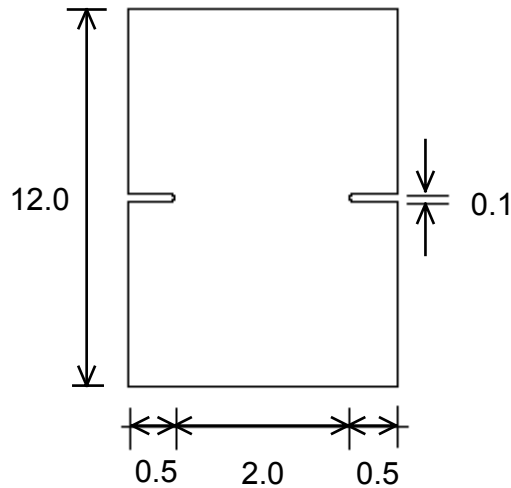


Figure 7 - Double-edge crack specimen for tensile test of concrete. 28 days of age. Thickness 0.75 to 1.5 inches. Units inch

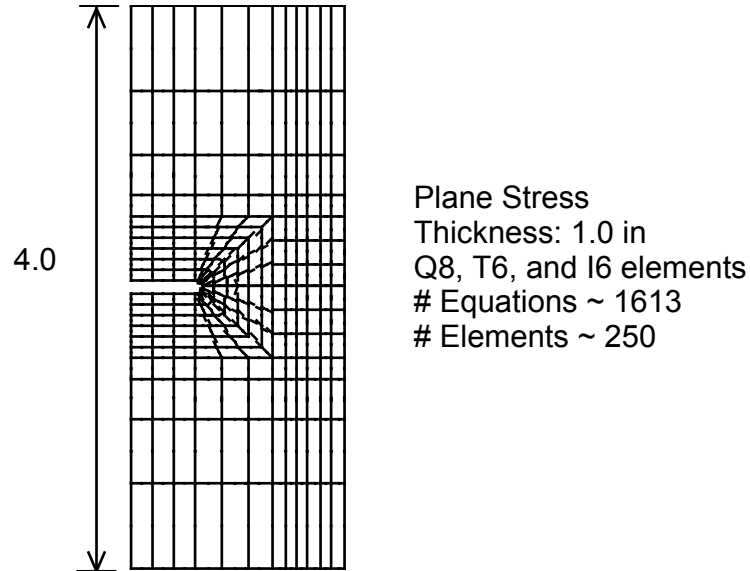


Figure 8 - Finite element model using half symmetry.

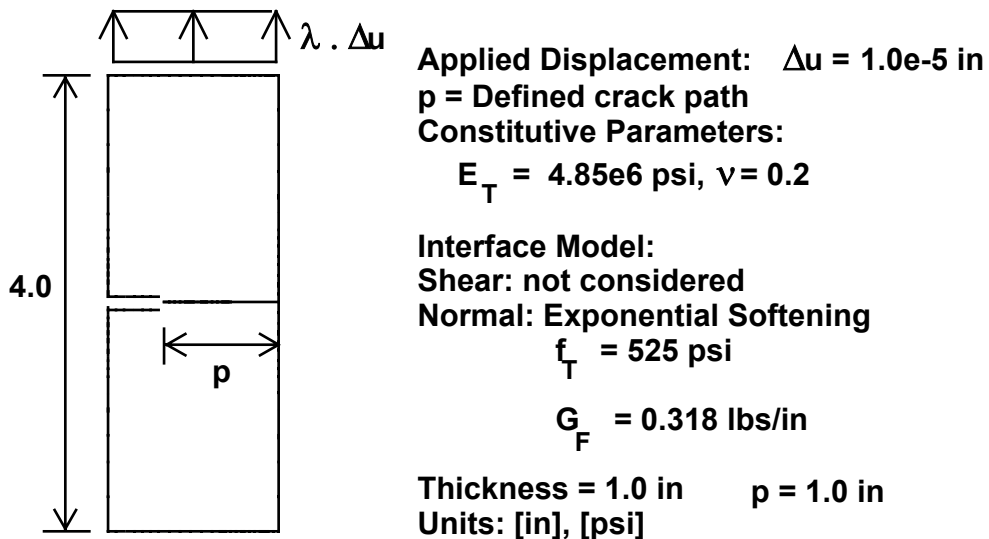


Figure 9 - Defined crack path (DP) analysis with applied displacements at the top of the specimen. Bottom is fixed.

The defined crack path analysis is considered first (Figure 9). A line starting from the notch and ending at the plane of symmetry defines the crack path. Interface elements which incorporates the exponential softening behavior are placed along this line. The position of the fictitious crack tip is estimated from the deformed configuration. Therefore, no crack stability criterion is needed. However, a displacement control analysis is employed in order to capture the softening branch of the force-displacement curve. The fracture process zone evolution obtained is shown in Figure 10. The process zone starts to move and strain localization takes place. For each load factor, the strain and average net stress can be recorded. The goal of the experiment was to compute the stress-strain curve for the specimen and illustrate strain localization. Because of the strain localization effect, the gauge length used to compute strains needs to be specified. In the experimental data a gauge length of 3.2 inches was considered. The average net stress is obtained by integration of the normal stresses along the line defining the crack path.

When the fracture length control scheme (ACC) is considered, the introduction of interface elements is done in an incremental way. The fictitious crack tip is moved forward with a consistent introduction of interface elements to describe the process zone. In this case, because of the nature of the approach, a crack stability criterion needs to be used in order to determine the load factor associated to the particular process zone configuration. The analysis is performed under fracture length control and, therefore, the softening branch of the load-displacement curve can be estimated independent of the way the loading is considered. In this analysis, the loading is defined by a uniform applied traction at the top and bottom of the specimen (Figure 11). The fracture process zone evolution (Figure 12) shows that the maximum load is yet to be achieved when the fictitious tip reaches the plane of symmetry (or the boundary of the model). This means that the fracture process zone has developed all along the ligament, but the specimen still has some load capacity. Unfortunately, the ACC approach cannot go beyond this point because the fictitious crack tip reaches the boundary of the model. From this point on the specimen ligament is completely damaged and the fictitious crack tip notion cannot be used. The increase of the average net stress with respect to the fictitious crack tip position can be obtained only up to this point (Figure 13).

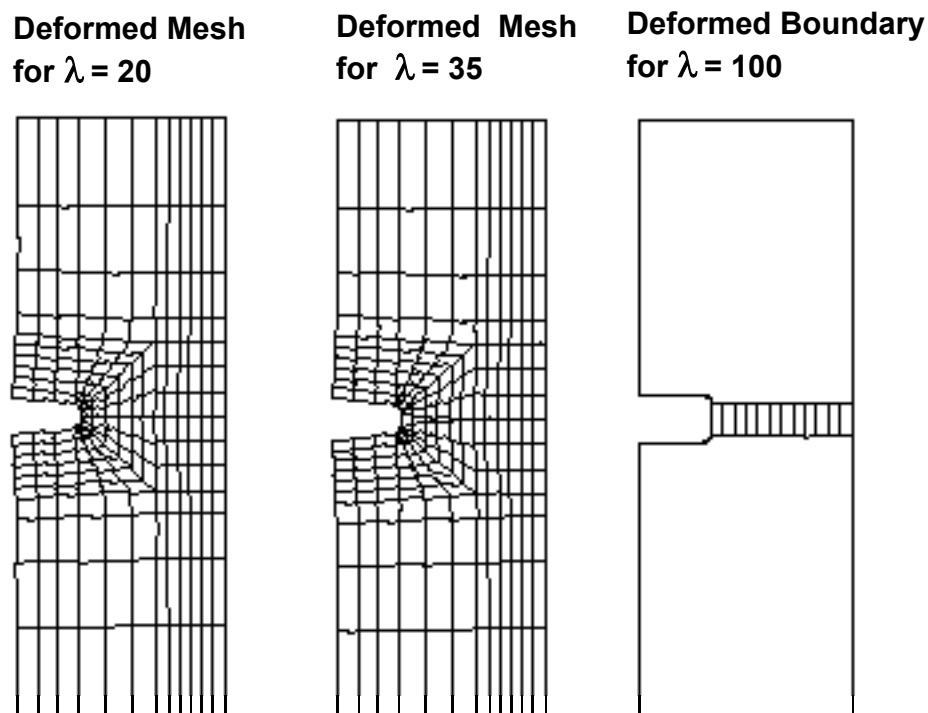


Figure 10 - Fracture process zone evolution with later strain localization effect for defined crack path (DP) analysis.

A comparison between the experimental data and the computed results through DP and ACC approaches is presented next (Figure 14). As mentioned before, the ACC analysis cannot go beyond the point where the fictitious crack tip reaches the boundary of the model. However, up to this point the results are consistent to experimental observations. Two gauge lengths have been used to compute the strains from DP analysis. One important aspect to be observed, though, is that the computed strains increase for a shorter gauge length. This characterizes strain localization. The strains will ultimately localize within a narrow process zone, with the upper and lower parts of the specimen behaving almost like rigid bodies. In general, both the DP and ACC strategies provided good agreement with the experimental data.

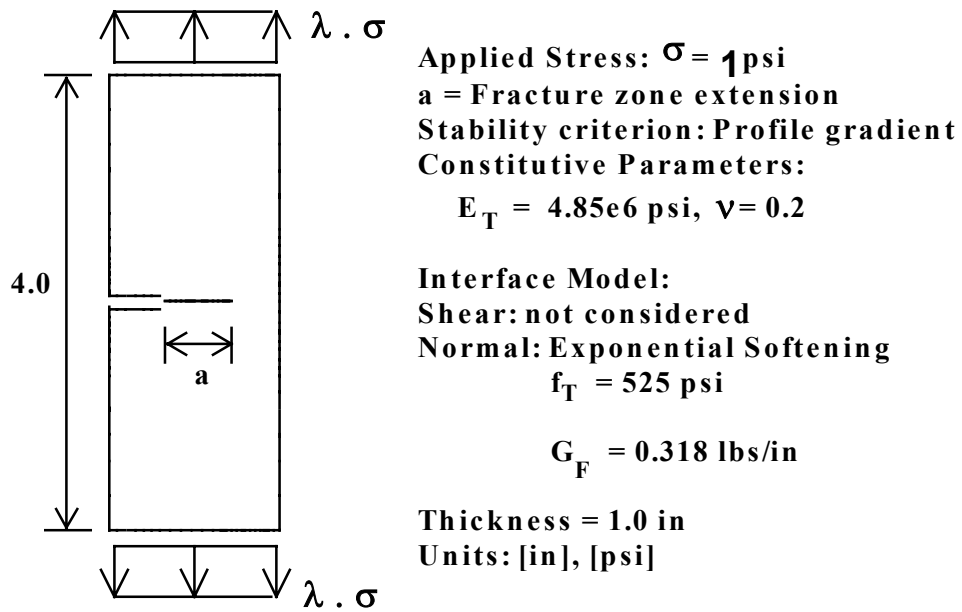


Figure 11 - Arbitrary, cohesive crack (ACC) analysis for applied uniform stress at the top and bottom of the specimen.

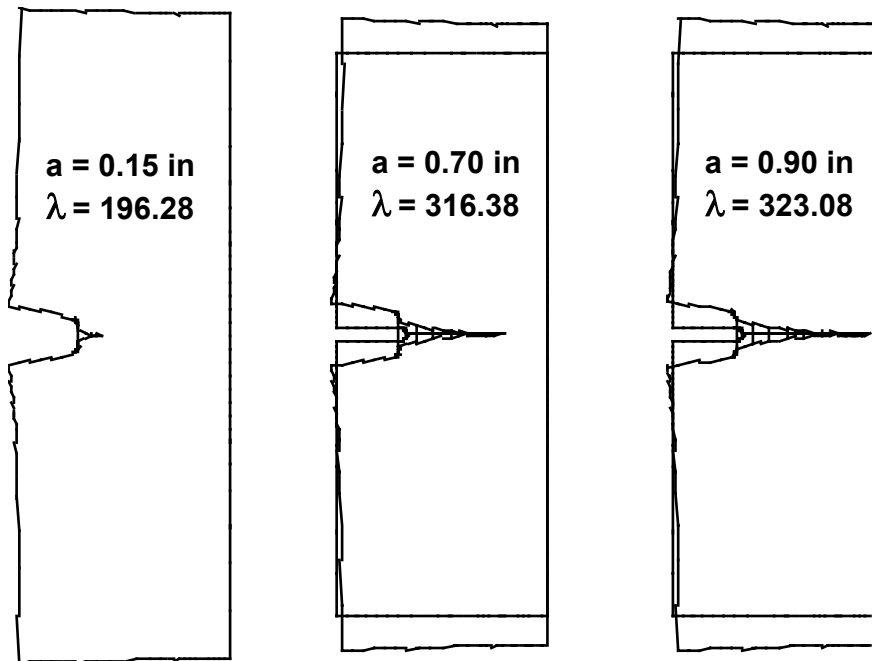


Figure 12 - Process zone evolution for arbitrary, cohesive crack (ACC) analysis.

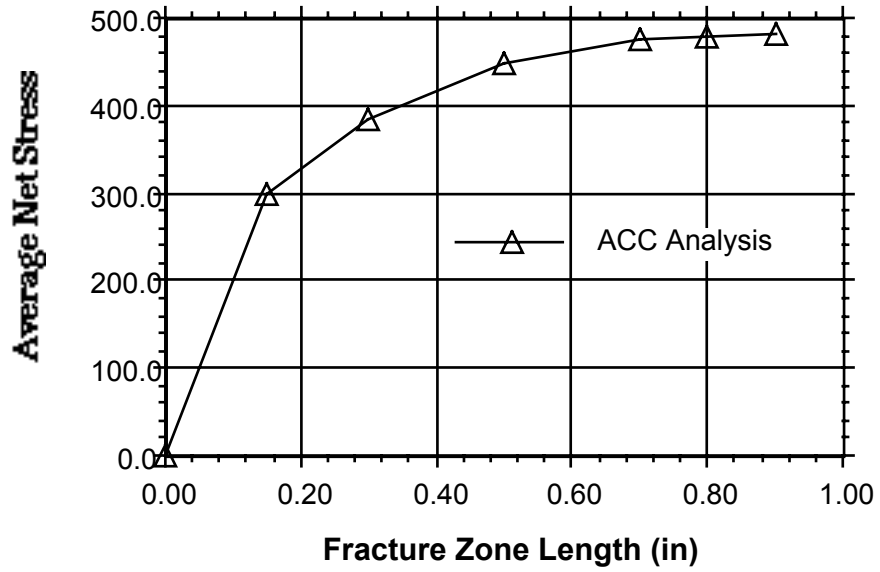


Figure 13 - Fictitious crack tip propagation from ACC analysis. Net Stress in psi.

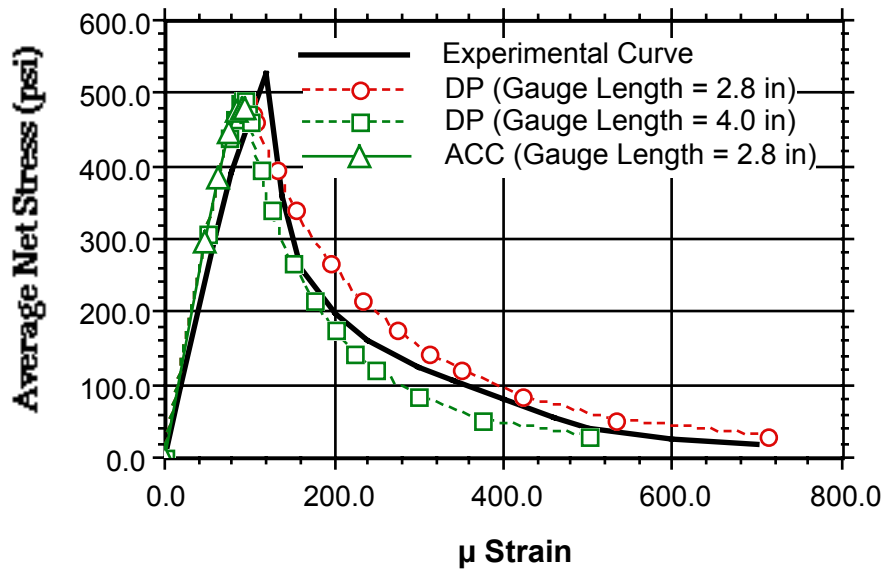


Figure 14 - Average net stress versus strain curves comparison. Net Stress in psi.

6.2. Concrete Beam - SEN(B) Configuration

The SEN(B) specimen of Figure 15 illustrates how size effects may completely change the behavior of the specimen, and how the DP and ACC strategies model all these possibilities. The relative geometry of the beam is preserved, while beam height varies from 50 mm to 300 mm. Plane stress is assumed. No initial notch is considered. Material properties and the interface softening model used in this analysis are presented in Figure 15.

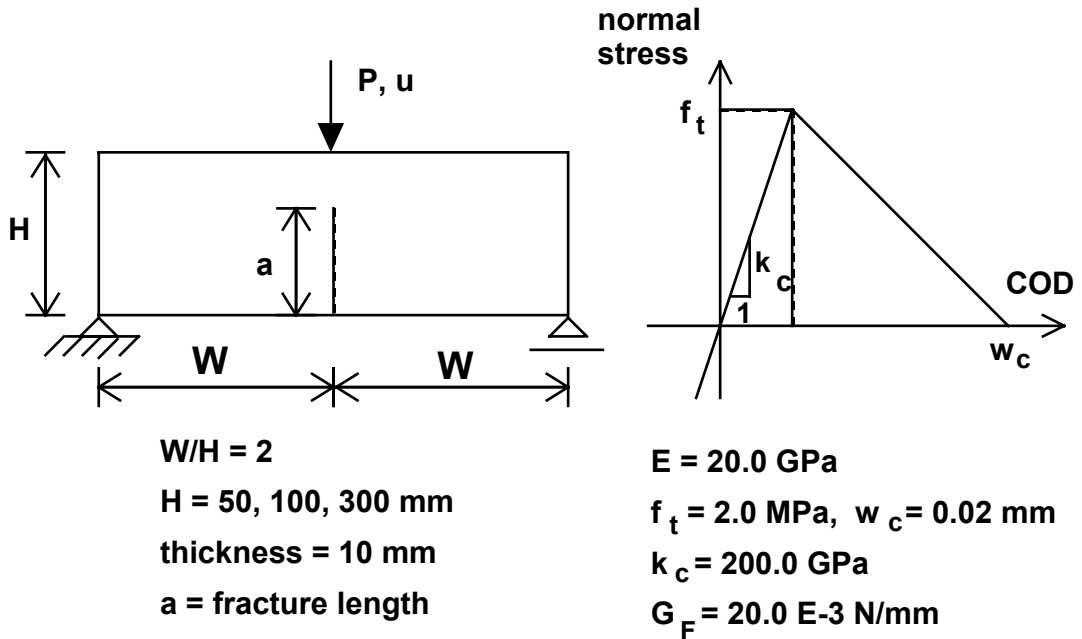


Figure 15 - SEN(B) Geometry, Interface Softening Model, and Material Parameters.

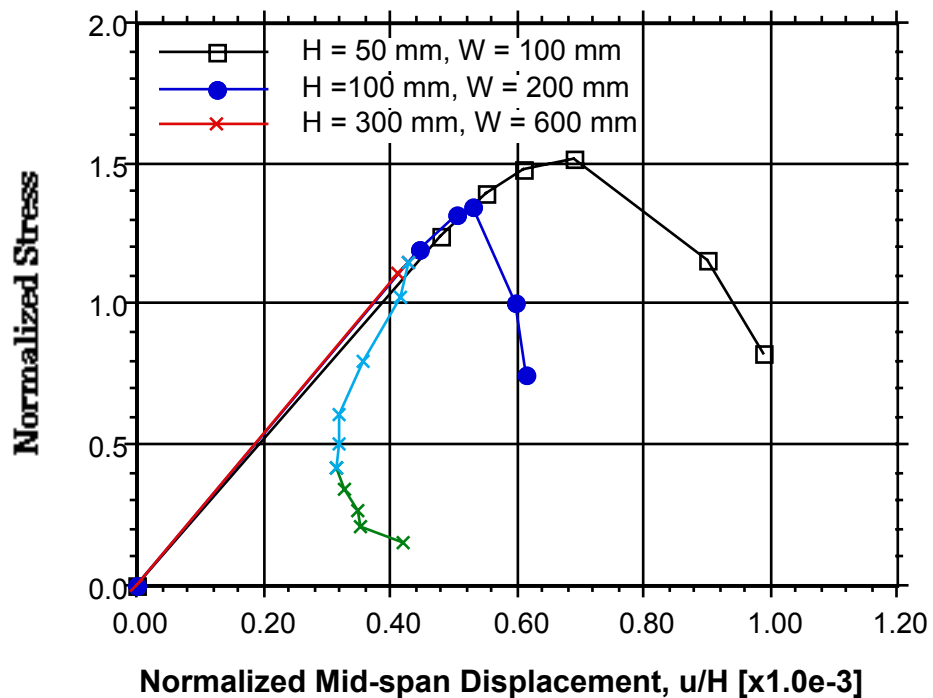


Figure 16 - Predicted load-displacement curves for the SEN(B) analyses.

The ACC approach is used to model the fracture process. Figure 16 shows predicted non-dimensional load-displacement curves for the SEN(B) structure. Normalized stress is the ratio σ_N/f_t , where σ_N is the beam theory extreme fiber tensile stress at midspan for the uncracked beam. It is clear that the present strategy is able to detect moderate and severe softening and, importantly, a snap-back instability. Fracture process zone length, as pointed out before, is an increasing function under the user's control (Figure 17).

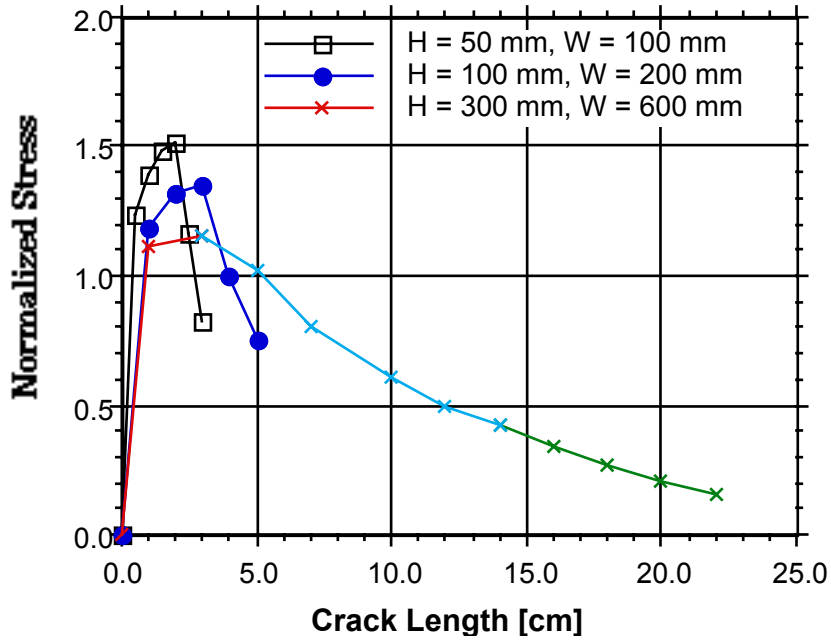


Figure 17 - Total crack length (a) (true crack plus fracture process zone) versus normalized stress for SEN(B) analyses.

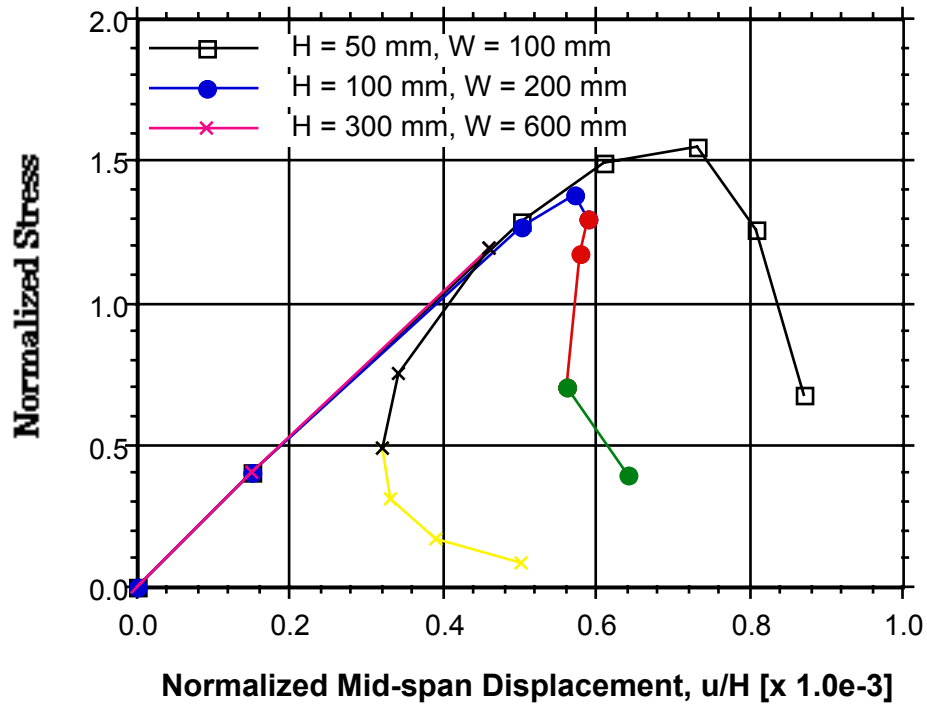


Figure 18 - Load-displacement curves computed through the Influence Method.

Experience with this example problem indicates that there can be extreme sensitivity in load factor to small variations in the slope of the COD profile on the decreasing branch of the load versus displacement curves. Consequently, the load-displacement curve along the softening branch (post-peak) is not accurate. However, the influence method provides an accurate solution for this problem (Figure 18). When these results are compared to those of the ACC analysis, it becomes clear that the results along the softening path do not match properly for all the specimen geometric configurations. Interestingly, the snap-back behavior of the largest beam ($H = 300$ mm) shows good agreement with the solution provided by the influence method. However, the loading paths up to the maximum loads are exactly the same. Therefore, the predictions of the load capacity of the beams agree very well.

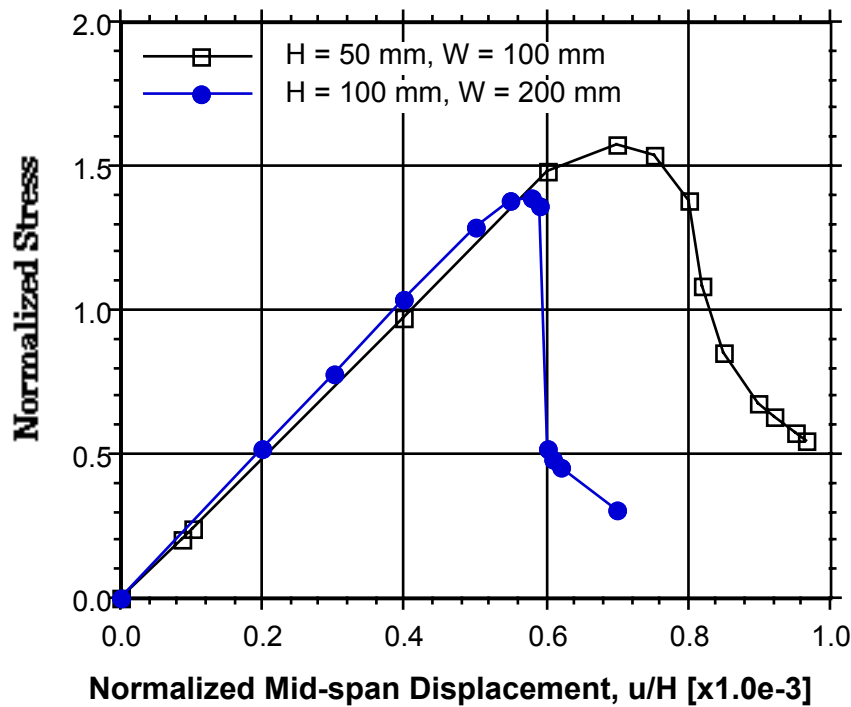


Figure 19 - Load-displacement curves for defined crack path (DP) with applied displacements.

The (DP) approach provides more insight to the problem. This approach, like the influence method, is limited to the cases where the crack or fracture process trajectory is known *a priori*. For the present problem, however, that is exactly the case. Interface elements with the same constitutive model (Figure 15) are placed along the crack path. The beam is analyzed under displacement control. An initial mid-span displacement (u) of $0.0001H$ (mm) is considered. The extension of the fracture process zone is modeled by applying a load factor to the initial displacement. The mid-span load (P) associated to the applied displacements are obtained from the support reactions. The normalized stress versus normalized mid-span displacement curve can be then generated (Figure 19). Only the two smaller beams have been analyzed. Because displacements control the analysis snap-back cannot be fully captured. There is a sudden jump in the curve in these circumstances (Figure 19 for $H = 100$ mm). However, for the other portions of the curves, including the softening branch, the results show very good agreement with ones from the influence method. This indicates that the interface elements are performing properly. Therefore, the post-peak accuracy problems observed when ACC is used are not due to the interface behavior.

The crack or fracture process zone opening profiles may shed some light on the problem. The crack opening profiles, for different load factor levels, obtained from the DP analyses are shown in Figures 20 and 21. It should be noticed that the load factor controls the mid-span displacement values.

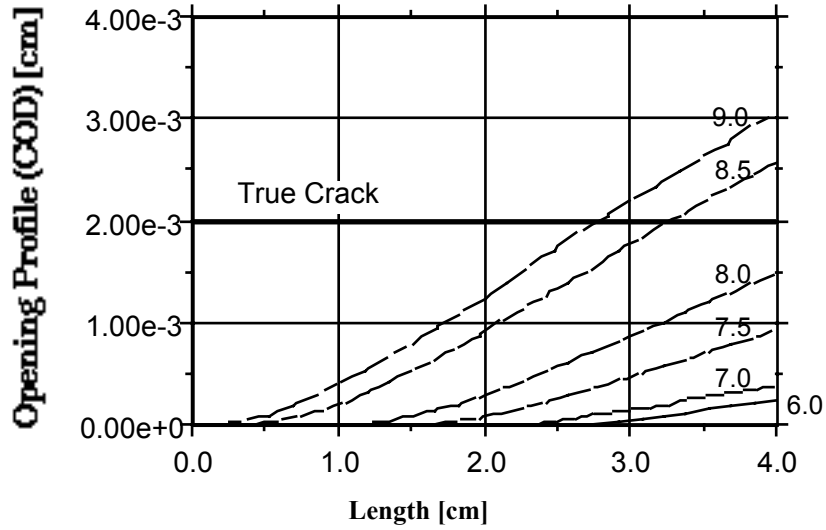


Figure 20 - Crack opening profile for different levels of load factors from DP method (H=50, W=100 mm).

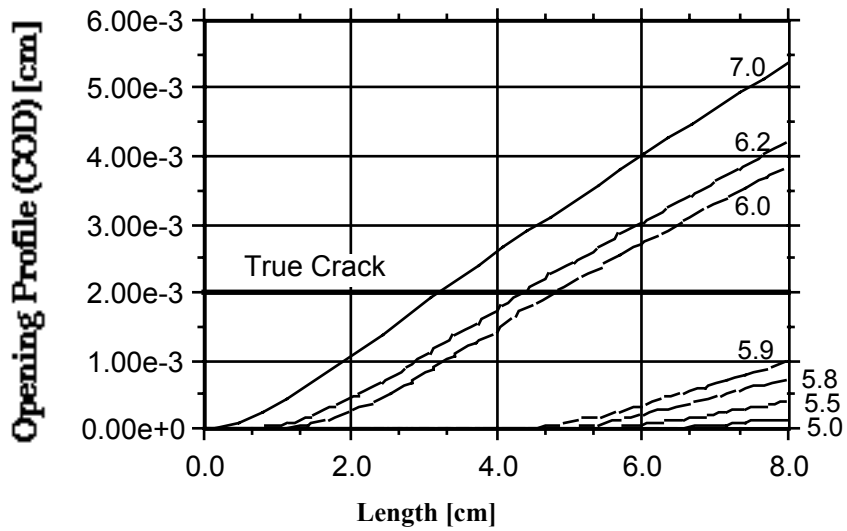


Figure 21 - Crack opening profile for different levels of load factors from DP method (H=100, W=200 mm).

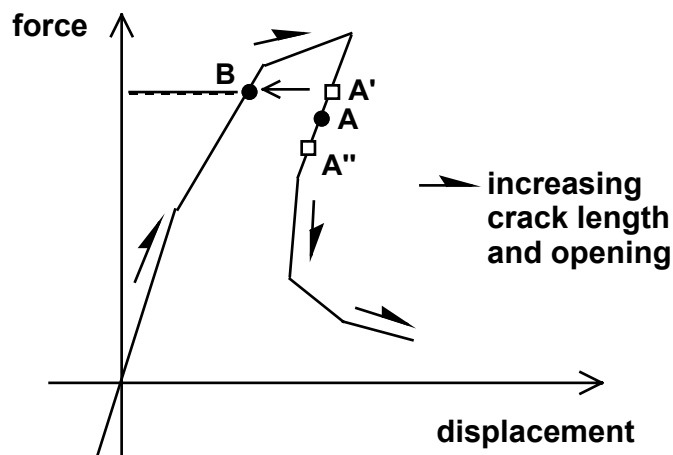


Figure 22 - Schematic behavior of search for equilibrium in the ACC approach.

As can be seen, for the first beam (Figure 20) the opening smoothly increases for increasing values of the mid-span displacement (u). For the other beam (Figure 21), a sudden jump is obtained when the load factor reaches a value around 5.9. However, the crack opening keeps increasing during the fracture zone propagation with an eventual true crack extension. This increase of crack opening is not enforced in the ACC approach. This is the main reason for the poor accuracy of the post-peak branches of the load-displacement curves (Figure 16).

An improvement of the proposed ACC approach can be achieved by providing a material model update for the pre-existing interface elements so that crack closing is precluded. This would force the iterative equilibrium solver to find a load factor that would keep the fracture zone opening profile continuously increasing, consequently finding a post-peak solution for the problem (Figure 22). The inaccuracy comes from the fact that the interface element can handle both closed and open configurations. The computation of the load factor follows a bracketing procedure. To determine the load factor associated with point A (Figure 22) estimate values for upper and lower points (A' and A'') are necessary. As mentioned before, the load search procedure starts from an open crack profile without the consideration of the cohesive forces. The cohesive forces are then introduced and the crack profile closes until the stability criterion is satisfied. This will permit the computation of a load factor associated to a configuration in which the fictitious crack tip is ahead of the one established (point A''). The load factor is then slowly decreased. Eventually, the algorithm may decide to close the crack more than necessary to find a lower bracket for the solution (point A'). When this situation is reached, there exists an infinite number of possible equilibrium configurations associated with the load-displacement curve between points B and A' (Figure 22). If no constraint is imposed on DR, it solves the problem by jumping to point B. This effect compromises the bracketing process causing the computation of inaccurate results. By enforcing an increasing crack profile on DR, the point A' could be then evaluated. However, the proposed strategy in its present implementation is still very useful to estimate the load capacity of the structure and also to detect any softening condition.

7. Summary

The application of the fictitious cohesive crack model has been investigated for 2D problems. Different strategies to solve the problem has been presented. The use of nonlinear interface elements to model the cohesive zone softening behavior has been detailed.

A new system for simulating the initiation and propagation of arbitrary, cohesive cracks has been presented. The system integrates geometrical and mesh representation, finite element, non-linear solution, non-linear fracture mechanics, and automatic remeshing techniques on an engineering workstation behind a graphical user interface. This system computes a load factor that simultaneously satisfies global equilibrium and a local crack stability criterion for a given fictitious crack length. A local criterion based on zero-slope of the COD profile at the fictitious crack tip may be used. The dynamic relaxation non-linear solution technique is capable of handling highly non-linear behavior, including snap-back, making it very general and powerful. This system is heir to over a decade of work in modeling crack initiation and propagation in concrete and rock. It has been designed with data structure and code architecture in mind to allow it to receive new constitutive formulations and solution techniques gracefully.

The application of the mentioned strategies has been illustrated in the example problems. The limitations and advantages of each strategy have been explained. An important improvement to the ACC strategy has been also suggested.

8. References

- [Bazant 1983] Bazant, Z.P. and Oh, B., "Crack band theory for fracture of concrete," *Materials and Structures*, Vol.16, N° 93, (1983), pp.155-177.
- [Becher 1988] Becher, P.F., Hsueh, H., Angelini, P. and Tiegs, T.N., "Toughening behavior in whisker-reinforced ceramic matrix composites," *Journal of American Ceramic Society*, Vol. 71[12], (1988), pp.1050-1061.

- [Bittencourt 1993] Bittencourt, T.N., "Computer Simulation of Linear and Nonlinear Crack Propagation in Cementitious Materials," *Ph.D. Thesis*, Cornell University, (1993).
- [Bocca 1991] Bocca, P., Carpinteri, A. and Valente, S., "Mixed mode fracture of concrete," *International Journal of Solids and Structures*, Vol.27, N° 9, (1991), pp.1139-1153.
- [Carpinteri 1984] Carpinteri, A., "Interpretation of the Griffith instability as a bifurcation on the global equilibrium," *Application of Fracture Mechanics to Cementitious Composites*, NATO-ARW, (1984), pp.287-316.
- [Gopalaratnam 1985] Gopalaratnam, V.S., and Shah, S.P., "Softening response of plain concrete in direct tension," *ACI Journal*, (1985), pp.310-323.
- [Hellier 1987] Hellier, A.K., Sansalone, M., Carino, N.J., Stone, W.C. and Ingraffea, A.R., "Finite-element analysis of the pullout test using a nonlinear discrete cracking approach," *Cement, Concrete, and Aggregates*, Vol.9, N° 1, (1987), pp. 20-29.
- [Hillerborg 1976] Hillerborg, A., Modeer, M., and Petersson, P-E., "Analysis of crack formation and crack growth in concrete by means of fracture mechanics and finite elements," *Cement and Concrete Research*, Vol.6, (1976), pp.773-782.
- [Ingraffea 1984a] Ingraffea, A.R. and Gerstle, W.H., "Non-linear fracture models for discrete crack propagation," *Application of Fracture Mechanics to Cementitious Composites*, NATO-ARW, September 4-7, (1984), pp.171-207.
- [Ingraffea 1984b] Ingraffea, A.R., Gerstle, W.H., Gergely, P. and Saouma, V., "Fracture mechanics of bond in reinforced concrete," *Journal of Structural Engineering*, ASCE, Vol.110, N° 4, (1984), pp.871-889.
- [Ingraffea 1987] Ingraffea, A.R., "Theory of Crack Initiation and Propagation in Rock," Chapter 3 in *Rock Fracture Mechanics*, B. Atkinson, editor, Academic Press Inc., (1987).
- [Jenq 1985] Jenq, Y. and Shah, S.P., "Two parameter fracture model for concrete," *ASCE, EMD*, Vol.11, N° 10, (1985).
- [Llorca 1990] Llorca, J. and Elices, M., "Fracture resistance of fiber-reinforced ceramic matrix composites," *Acta Metallurgica*, Vol. 38[12], (1990), pp.2485-2492.
- [Llorca 1991] Llorca, J. and Steinbrech, R.W., "Fracture of alumina: an experimental and numerical study," *Journal of Material Science*, Vol. 6, (1991), pp. 383-390.
- [Mai 1991] Mai, Y.M., "Fracture and fatigue of non-transformable ceramics: the role of crack-interface bridging," *Fracture Processes in Concrete, Rock and Ceramics*, Edited by Van Mier, J.G.M., London, (1991).
- [Petersson 1981] Petersson, P-E., "Crack growth and development of fracture zones in plain concrete and similar materials," *Report TVBM-1006/1-174*, Division of Building Materials, Lund Institute of Technology, Lund, Sweden, (1981).
- [Rödel 1990] Rödel, J., Kelly, J.F. and Lawn, B.R., "In situ measurements of bridged crack interfaces in the scanning electron microscope," *Journal of American Ceramic Society*, Vol. 73[11], (1990), pp.3313-3318.
- [Samet 1984] Samet, H., "The quadtree and related hierarchical data structures," *ACM Computer Surveys*, Vol.16[2], (1984).
- [Saouma 1982] Saouma, V.E., Ingraffea, A.R. and Catalano, D.M., "Fracture toughness of concrete: K_{IC} revisited," *Journal of Engineering Mechanics Division*, ASCE, Vol.108, N° EM6, (1982), pp.1152-1166.
- [Shah 1989] Shah, S.P., "Whither fracture mechanics for concrete," Keynote Lecture, *Fracture of Concrete and Rock: Recent Developments*, Edited by S.P.Shah, S.E.Swartz, and B.Barr, Elsevier Science Publishers LTD, (1989), pp.1-4.
- [Swanson 1987] Swanson, P.L., Fairbanks, C.J, Lawn, B.R, Mai, Y.W., and Jockey, B.J., "Crack interface grain bridging as a fracture resistance mechanism in ceramics: experimental study on alumina," *Journal of American Ceramic Society*, Vol. 70[4], (1987), pp.279-289.
- [Swenson 1991] Swenson, D.V., Ingraffea, A.R., "The collapse of the schoharie creek bridge: A case study in concrete fracture mechanics," *Int. Journal of Fracture*, Vol. 51, (1991), pp.73-92.
- [Underwood 1983] Underwood, P.G., "Dynamic relaxation," *Computational Methods for Transient Analysis*, Edited by T. Belytschko and T. J. R. Hughes, Elsevier Science Publishers, (1983), pp. 245-265.
- [Vekinis 1990] Vekinis, G., Ashby, M.F. and Beaumont, P.W.R., "R-curve behavior of Al_2O_3 ceramics," *Acta Metallurgica*, Vol. 38[6], (1990), pp.1151-1162.

- [Wawrzynek 1987a] Wawrzynek, P.A. and Ingraffea, A. R., "Interactive finite element analysis of fracture processes: An Integrated Approach," *Theor. & Appl. Frac. Mech.*, (1987).
- [Wawrzynek 1987b] Wawrzynek, P.A. and Ingraffea, A.R., "An edge-based data structure for two-dimensional finite element analysis," *Engn. with Computers*, 3, (1987), pp.13-20.
- [Wawrzynek 1987c] Wawrzynek, P.A., Boone, T., and Ingraffea, A.R., "Efficient techniques for modeling the fracture process zone in rock and concrete," *Proc. of the Fourth International Conference on Numerical Methods in Fracture Mechanics*, March 23-27, (1987), San Antonio, Texas, A.R. Luxmoore, D.R.J. Owen, Y.S. Rajapakse, and M.F. Kanninen, Editors, pp. 473 - 482.
- [Wawrzynek 1991] Wawrzynek, P.A., "Discrete modeling of crack propagation: theoretical aspects and implementation issues in two and three dimensions," *Ph.D. Thesis*, Cornell University, (1991).